ORIGINAL ARTICLES

Size dependence of inherent image quality of a 2nd generation dual source CT scanner

Yakun Zhang[1], Justin Solomon[2], Ehsan Samei[1,2,3]

1. Department of Radiology, Duke University Medical Center, Durham, NC, USA. 2. Medical Physics Graduate Program, Duke University, Durham, NC, USA. 3. Departments of Physics, Biomedical Engineering, and Electrical and Computer Engineering, Duke University, Durham, NC, USA

Correspondence: Yakun Zhang. Address: 2424 Erwin Rd, Suite 302, Durham, NC 27705, USA.
Email: yakun.zhang@duke.edu

Received: August 31, 2015 **Accepted:** November 9, 2015 **Online Published:** November 20, 2015
DOI: 10.5430/ijdi.v3n1p40 **URL:** http://dx.doi.org/10.5430/ijdi.v3n1p40

Abstract

The fast developing CT technologies have complicated the protocol optimization process. Since there are increasing numbers of free parameters that can be adjusted, it is imperative to know exactly how these parameters affect the image quality. This paper examines the effect of varying dose level, tube voltage, reconstruction methods and the AEC function on the CT image quality across different sizes. A size varying phantom, consisting of five cylindrical tiers, was used. To assess the image quality, task transfer function (TTF), noise power spectra (NPS), contrast, and detectability index was computed and compared across sizes. It was found that from small to large size, detectability increased more as the dose increased. When the CTDIvol increased from 0.7 to 22.6 mGy, the detectability for the smallest size section increased by four fold but increased by eight fold for the largest section. Low tube voltage exhibited superior detectability and contrast for all sections, especially for the small size sections, where detectability doubled for the smallest section when tube voltage decreased from 120 kV to 80 kV. TTF curves showed considerable dependence on size, but more pronounced dependence on reconstruction techniques. In conclusion, small size phantoms were affected very differently from large size phantoms by dose levels, reconstruction methods, and tube voltage selection. Low tube voltage and iterative reconstruction technique can deliver superior image quality for small patients. Due to beam hardening and substantially increased noise at low tube voltage for large patients, high tube voltage is still recommended for large patients to retain image quality.

Keywords

Image quality, Computed tomography, Noise

1 Introduction

In the past few decades, commercial computed tomography has developed from a single slice head scan taking 2.5 hours, to multi-detector high resolution scans that can depict the anatomy of a beating heart. It has truly revolutionized the medical field. An estimated 62 million CT scans per year were conducted in the United States in 2006, of which 6.5% were done on children [1]. It is well understood that children have more radiosensitive tissues and organs, and longer life span for cancerous tumor to develop. Many efforts have been jointly contributed from medical physicists, radiologists, and technologists to raise awareness in pediatric imaging [2]. One remarkable effort was the founding of the Image Gently

Campaign, which promotes the justification for and optimization of pediatric CT imaging. To optimize pediatric CT protocols, a comprehensive understanding of the effect of patient size on image quality is desirable.

New CT systems usually come with many advanced applications to help to reduce radiation, such as different tube voltage selection and iterative reconstructions. Individually, each has been studied intensively before leading to the clinical application [3-10]. Lower tube voltage can provide better contrast because iodine preferentially absorbs much more photons at low tube voltage, but at lower tube voltage, images can be undesirably noisy [8-11]. Iterative reconstructions have been proven to reduce radiation dose notably, but can also alter the noise texture and obscure potential lesions of interest against a "waxy appearance" [5, 7, 11, 12]. To optimize protocols, these tradeoffs should be carefully and conjunctively considered. Inspired by this, our study focused on how size affects image quality with different imaging parameters using a second generation dual source CT scanner (SOMATOM Definition Flash, Siemens Healthcare). Some studies have reported the image quality from this new CT [5, 11, 13]. However, these studies focused on one particular technique, such as varying tube voltage, varying mAs, or comparing reconstruction methods. The purpose of this investigation is to comprehensively study the inherent image quality of a state of the art CT scanner using a size varying phantom.

2 Methods

2.1 The phantom and data collection

A size varying phantom was used (Mercury Phantom 3.0) [14]. This phantom consists of five cylindrical tiers, diameters 12 cm, 18 cm, 23 cm, 30 cm, 37 cm, with tapered connecting pieces. There are two sections within each tier, one with inserts and one without inserts, meant for characterization of the spatial resolution and noise properties respectively. The background material is polyethylene; the inserts are made from five different materials, including iodine concentration (8.5 mgI/cc), polystyrene, bone equivalent, water equivalent, and air. All inserts are located at the same radial distance (5 cm) to the transaxial center except for the smallest section where the inserts are closer to the center (3.3 cm).

The phantom was imaged on a second generation dual source CT scanner (SOMATOM Definition Flash, Siemens Healthcare). There are two X-ray tubes and detectors on this scanner. Both sources are enabled during applications including cardiac modes, high-pitch modes, and dual energy modes. In our experiments, only one tube and the larger detector was used. The collected images can be categorized into three data groups. The first group was with 120 kV and six dose levels. The CTDIvol values were 0.7, 1.4, 2.8, 5.7, 11.5, 22.6 mGy. The raw data was reconstructed both with FBP and SAFIRE 3, 4, 5. The second group was imaged at four different tube voltage levels (80, 100, 120, 140 kV), with matched CTDIvol of approximately 2.8 mGy. The third group used the tube current modulation (CareDose 4D, Siemens Healthcare) at three dose levels with 120 kV, where average CTDIvol was matched to be 1.4, 2.6, 5.7 mGy. Other image parameters are shown in Table 1.

Table 1. Data acquisition parameters

Items	
Reconstruction FOV	40 cm
Reconstruction method	FBP, SAFIRE 3, 4, 5
Slice thickness	0.625 mm
CTDIvol	0.7, 1.4, 2.8, 5.7, 11.5, 22.6 mGy
Tube current modulation setting	Reference mAs with CTDIvol of approximately 1.4, 2.8, 5.7 mGy
Pitch	1
Rotation time	1 s

2.2 Image analysis

Several image quality metrics were employed, including task transfer function (TTF) for spatial resolution [15], NPS for noise performance, contrast, as well as a detectability index which incorporates the resolution, contrast and noise properties into a single metric. The calculation of each one is detailed in the following.

The TTF and contrast were computed using the iodine concentration rod insert. A small rectangular ROI was drawn around the insert, then the weighted center (the center of mass) was found. The distance from the pixels in the ROI to the center was calculated and plotted against the pixel value. This yields an edge spread function, which was differentiated to calculate the line spread function (LSF). After smoothing the LSF with a Hann window, the Fourier transform was performed to obtain the TTF of the iodine insert [15]. Contrast was simply calculated as the subtraction of the insert HU and background HU.

The NPS was computed from the uniform section of each tier. A ring shaped ROI was used to exclude the middle assembly rod. The ROI sizes were chosen to be the same across all tiers for a fair comparison. Each ROI was first fitted into a second order polynomial fit, which was subtracted for the original ROI to obtain a noise map. Since the ROI was relatively small, the noise was assumed to be wide-sense stationary. Two dimensional autocovariance was estimated from the ROI, and the Fourier transform was performed to obtain a 2D NPS map. Assuming in-plane isotropy, the 1D NPS was computed by radially averaging the 2D NPS [11].

While TTF, contrast, and NPS capture parts of image quality, a singular metric is used to incorporate all of them. The task specific non-prewhitening observer model was used to calculate a detectability index d' [16]:

$$d'^2 = \frac{[\iint TTF^2(u,v)W_{task}^2(u,v)dudv]^2}{\iint nNPS(u,v)\,TTF^2(u,v)W_{task}^2(u,v)dudv}$$

where nNPS is the normalized NPS, and W_{task} is the task function. The task used in this study was a circular disk of 5 mm diameter. The contrast of the task was the contrast from the iodine insert.

3 Results

Figure 1 shows the image quality on different dose levels and reconstruction methods. All the detectability index measurements were performed on the iodine inserts. As expected, the detectability index was proportional to the dose level for all sizes. This is intuitively simple to understand–the more radiation, the less noise and the easier to detect an object. For the noise, Figure 1e plots the noise power spectra from the 23 cm section of the phantom, which clearly illustrated how noise magnitude increases as the dose level decreases. Figure 1a to 1d shows that iterative reconstruction had better detectability compared to FBP, and iterative strength five (SAFIRE 5) had the highest detectability. NPS from these different reconstruction methods also demonstrated that SAFIRE 5 had the least noise (see Figure 1e to 1h). While the magnitude of NPS informs the variance of image pixels, the shape of NPS informs the texture of an image. Normalized to the area under the NPS curve, nNPS was used to compare the difference of texture appearance at different dose levels (see Figure 1i to 1l). FBP based nNPS overlapped across all dose levels, which is expected because FBP is a linear reconstruction technique and thus the noise texture is expected to be independent of dose levels. The non-linear reconstruction techniques exhibited different noise texture response at low dose levels, especially for the SAFIRE 5 where nNPS for 0.7 mGy considerably shifted towards low frequencies. From the small to large section, detectability increased more as the dose increased. When the CTDIvol increased from 0.7 to 22.6 mGy, the detectability for the smallest size increased by four fold but increased by 8 fold for the largest section. This held true for the iterative reconstruction as well. The detectability was improved even more for the large size section.

 ISSN 2331-5857 E-ISSN 2331-5865

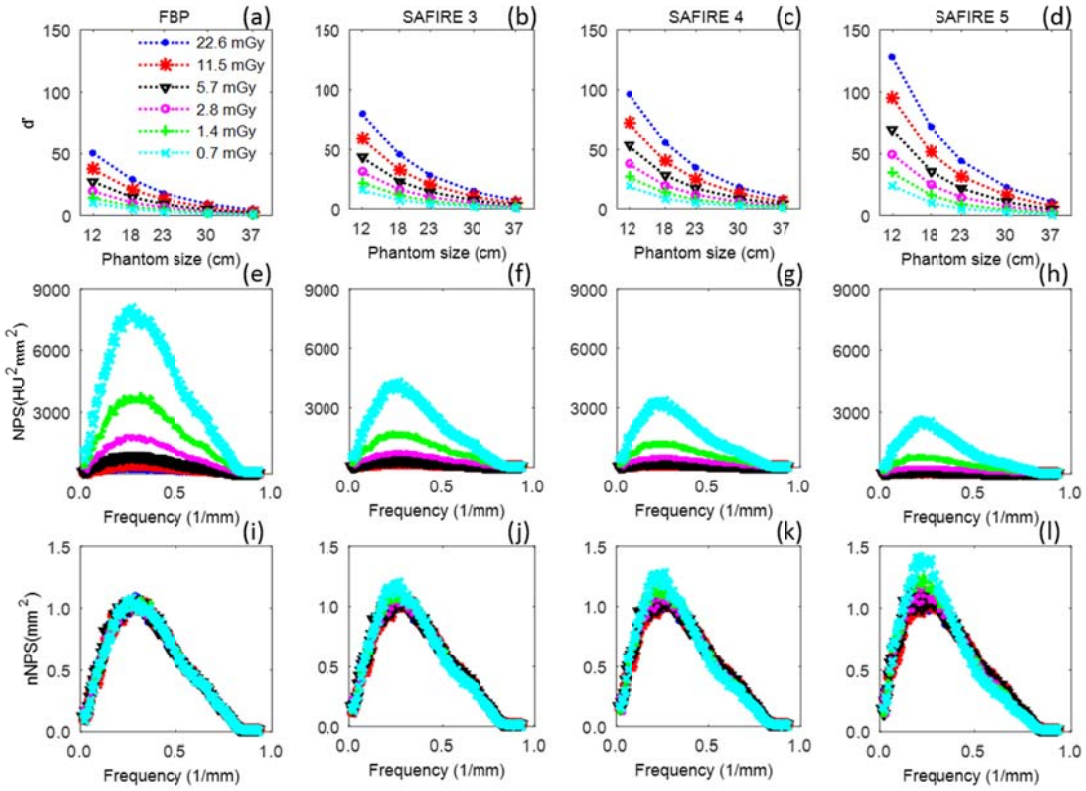

Figure 1. Image quality size dependence on dose levels and reconstruction methods. (a)-(d): Detectability indices for six dose levels, and FBP and SAFIRE reconstruction methods; (e)-(h): NPS from the uniform regions of the 23 cm section phantom for six dose levels and four reconstruction methods; (i)-(l): area-normalized NPS for six dose levels and four reconstruction methods

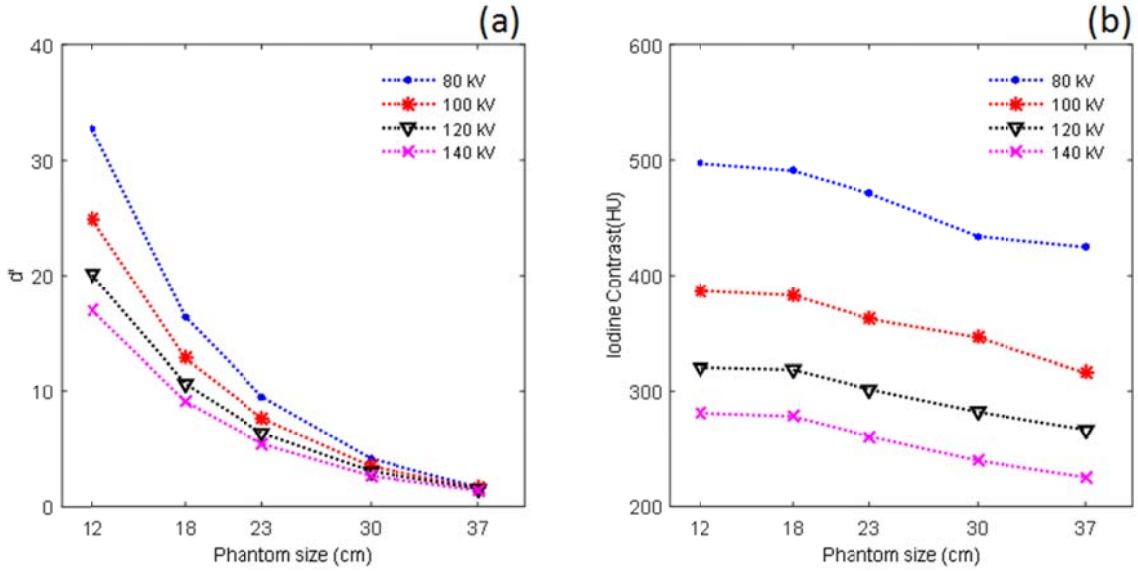

Figure 2. Image quality size dependence on tube voltages. (a): Detectability indices from FBP for four tube voltages; (b): Contrast for iodine insert from FBP for four tube voltages

Figure 2 shows the image quality size dependence on tube voltages. Since the results from IR were very similar to those for FBP, only FBP results are shown here. The data display a strong dependence of tube voltage on image quality–low tube voltage exhibited superior detectability and contrast for all sizes. For contrast, the lines from different tube voltages were almost parallel across sizes with an inverse proportional relationship between contrast and tube voltage. For detectability, tube voltage had a very large impact on the small section, but little impact on large size; detectability doubled for the 12 cm section, while remaining nearly unchanged for the 37 cm section. Contrast apparently did not contribute to this discrepancy among sizes since it increased for all sizes as noted before. The noise performance is tabulated in Table 2 across all sizes for the four tube voltages. Variances were similar for the same section at small sizes for the four tube voltages, but were considerably different for the large section 37 cm, with variance at 80 kV about 2.5 times that of 140 kV. The average frequency of NPS remained around 0.355 1/mm for all size and tube voltages besides the 37 cm section, where the frequency was considerably smaller compared to other sections.

Table 2a. Variance (HU2) from the uniform regions for four tube voltages

	12 cm	18 cm	23 cm	30 cm	37 cm
80 kV	177	675	1853	8076	35992
100 kV	186	667	1709	7616	21178
120 kV	196	675	1672	6723	15511
140 kV	211	704	1709	6420	14627

Table 2b. The average frequency (1/mm) of NPS for four tube voltages

	12 cm	18 cm	23 cm	30 cm	37 cm
80 kV	0.354	0.355	0.355	0.350	0.320
100 kV	0.354	0.354	0.356	0.354	0.319
120 kV	0.353	0.354	0.354	0.354	0.318
140 kV	0.353	0.355	0.354	0.356	0.323

Another important contributing factor to detectability is the spatial resolution response from the system. In this study, TTF was used to quantify this characteristic. Table 3 shows the frequency at 50% on the TTF curves for different reconstruction techniques, sizes and tube voltages; as an example, Figure 3 shows the TTF curves for iodine inserts at 120 kV. A considerable dependence on phantom size, but a more pronounced dependence on reconstruction techniques, was observed. As expected, IR displayed better resolution mostly. For FBP, the frequency remained similar across different tube voltages for sizes ranging from 12 cm to 30 cm, while contrarily for IR, the frequency generally increased proportionally with tube voltage for these sizes. Results from the 37 cm section had very different trending, which is largely due to the beam hardening effect.

Figure 4 shows the effect of AEC on the size varying phantom. This demonstrates another important usage of the Mercury Phantom, to assess the tube current modulation function of modern CT scanners. The average CTDIvol was purposefully matched to three dose levels. The detectability curves were flatter when AEC was applied, although not completely flat as might be anticipated for AEC based scans. This is a function of the specifics of the tube current modulation techniques applied.

4 Discussion

The fast developing CT technologies have complicated the protocol optimization process. Since there are growing variants that can be adjusted, it is imperative to know exactly how these parameters affect the image quality. This paper examines the effect of varying dose level, tube voltage, reconstruction methods and the AEC function for various sized phantoms on

 ISSN 2331-5857 E-ISSN 2331-5865

the CT image quality. The primary focus of this work is the detection of iodinated features, however, the results can be extrapolated to other features comprising high contrast in images.

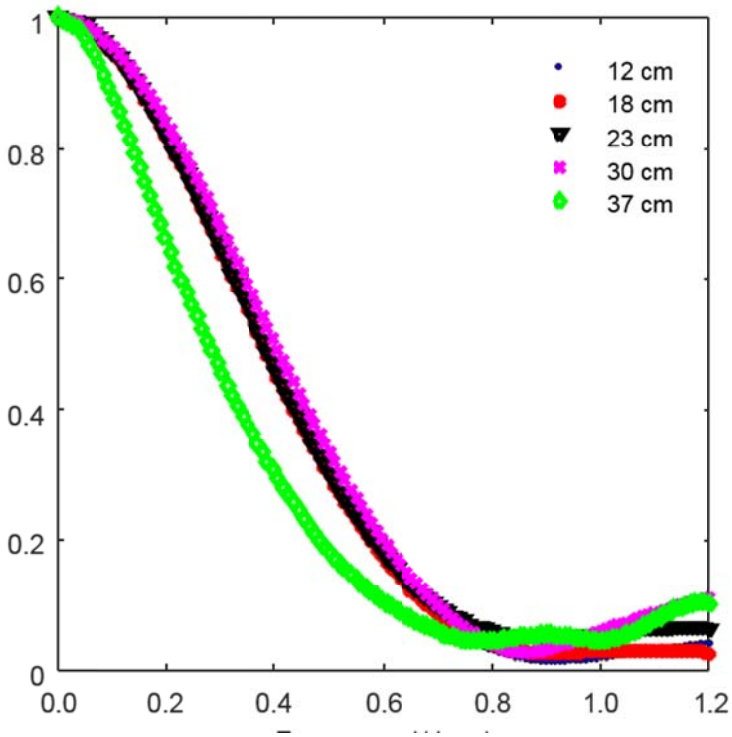

Figure 3. TTF curves for iodine inserts from FBP for all phantom sizes at 120 kV

Table 3. Frequency (1/mm) at 50% on the TTF curves for iodine inserts.

		12 cm	18 cm	23 cm	30 cm	37 cm
FBP	80 kV	0.355	0.332	0.332	0.335	0.291
	100 kV	0.355	0.332	0.332	0.335	0.271
	120 kV	0.355	0.352	0.332	0.356	0.291
	140 kV	0.355	0.332	0.332	0.356	0.291
	Average	0.355	0.337	0.332	0.346	0.286
Safire 3	80 kV	0.355	0.353	0.353	0.377	0.291
	100 kV	0.355	0.353	0.353	0.377	0.271
	120 kV	0.376	0.373	0.374	0.377	0.291
	140 kV	0.376	0.373	0.353	0.377	0.270
	Average	0.365	0.363	0.358	0.377	0.281
Safire 4	80 kV	0.355	0.353	0.353	0.377	0.290
	100 kV	0.355	0.353	0.374	0.377	0.271
	120 kV	0.376	0.373	0.374	0.398	0.270
	140 kV	0.376	0.373	0.353	0.377	0.270
	Average	0.365	0.363	0.363	0.382	0.276
Safire 5	80 kV	0.355	0.353	0.373	0.398	0.290
	100 kV	0.376	0.373	0.374	0.398	0.271
	120 kV	0.376	0.394	0.394	0.398	0.270
	140 kV	0.397	0.394	0.395	0.377	0.249
	Average	0.376	0.378	0.384	0.393	0.270

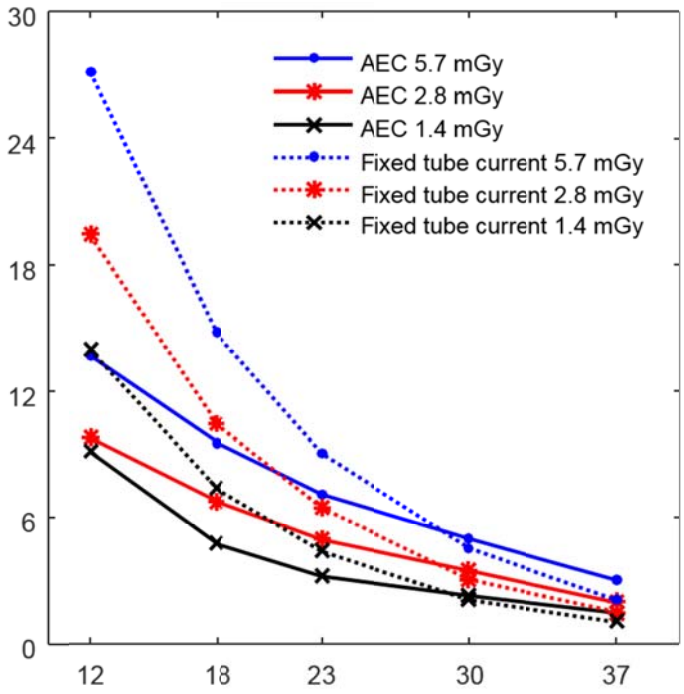

Figure 4. Detectability indices for AEC and fixed tube current acquisitions at three similar dose levels

It has been previously reported that the iterative reconstruction technique SAFIRE would not only alter the noise magnitude but also the noise texture, which was confirmed in this study [5]. What was also found was that SAFIRE changes the noise texture in different ways at different dose levels. Unlike the FBP where NPS remained similar regardless of the dose levels, NPS for SAFIRE exhibited dose dependency whereas for low dose levels, the NPS is shifted towards the low frequencies, especially when a high level of iterative strength is applied. This change is the reflection of the way noise regularization process is implemented during the image reconstruction. This process evaluates the contrast and analyzes edges in the image, then smooth the uniform area. Thus, different content of the images were smoothed differently resulting a change in the texture appearance. When the dose is extremely low, the inherent noise is very high; our results indicated that the reconstruction process smoothed the image more in this condition, resulting a more apparent change in noise texture. This effect has also been reported in other commercial iterative reconstruction techniques [7].

This study analyzed the effect of tube voltage on different sizes of phantoms. The results indicated that lower tube voltage yielded better image quality for small patients, which is consistent with previous research [10]. We explored several image quality metrics to have a thorough understanding of this effect. Contrast, very often used when discussing tube voltage, did not show much advantage for small patients. It increased almost the same percentage for all sizes when tube voltage is lowered from 140 kV to 80 kV. The TTF from the iodine inserts for each size remained relatively constant when the tube voltage was varied. This indicates that the spatial resolution of the CT scanner used in this study does not depend on the energy of the photons. The one metric that did change greatly was the noise. For the small size phantom, the noise magnitude was similar at 80 and 140 kV; however for the large size phantom, the noise magnitude at 80 kV was about 2.5 times of that of 140 kV. This means that there is a tradeoff between the contrast gain and noise. Yu el al have proposed a systematic way of selecting tube voltage for different size patients. Our work supported the need for implementing such a method.

The methods used in this study can be implemented to clinical protocol optimization. The Mercury phantom can be imaged using the clinical protocol with the six dose levels from this paper. The detectability of high contrast and low contrast features can be extracted from the acquired images, which can then be converted to operating characteristic curves [17]. These curves are functions of contrast, dose level, and patient size. For a targeted size and contrast object, to achieve a detection threshold, the necessary dose level can be determined for the particular protocol.

There are several limitations to this study. First, when analyzing noise, only a uniform phantom was used. Solomon and Samei have shown uniform phantoms are not enough for assessing noise performance of iterative reconstruction given that no anatomy is perfectly uniform. Considering the frequency shift from iterative reconstruction, it would be worth exploring the noise performance using textured phantoms at various sizes. Second, this work used only two kernels from one vendor. It is understood that the kernel choice can have a notable effect on the TTF and noise, and thus the detectability index. It is not feasible to examine every single kernel available, but some representative kernels can be studied using similar methods, which can aid in the clinical optimization of protocols. However, the general findings from this paper, frequency shift in NPS and tradeoff between contrast and noise for tube voltage, are still applicable clinically.

In conclusion, this work examined the image quality of a commercial CT scanner using a size varying phantom. The size dependence of image quality on dose levels, reconstruction methods, tube voltage, and AEC were studied. Small size phantoms were affected very differently from large size phantoms with dose levels, reconstruction methods, and tube voltage selection. In general, low tube voltage and SAFIRE can deliver superior image quality for small patients. Due to beam hardening and substantially increased noise at low tube voltage for large patients, high tube voltage is still recommended for large patients to retain image quality. The nonlinear iterative reconstruction shifted the noise power spectra towards low frequencies especially for the extreme low dose scans. The results from this study can be implemented to optimize clinical protocols for different size patients.

References

[1] Brenner DJ, Hall EJ. Computed tomography-an increasing source of radiation exposure. The New England journal of medicine. 2007; 357(22): 2277-84. PMid:18046031 http://dx.doi.org/10.1056/NEJMra072149

[2] Goske MJ, Applegate KE, Boylan J, *et al*. The 'Image Gently' campaign: increasing CT radiation dose awareness through a national education and awareness program. Pediatric radiology. 2008; 38(3): 265-9. PMid:18202842 http://dx.doi.org/10.1007/s00247-007-0743-3

[3] Baker ME, Dong F, Primak A, *et al*. Contrast-to-noise ratio and low-contrast object resolution on full- and low-dose MDCT: SAFIRE versus filtered back projection in a low-contrast object phantom and in the liver. AJR American journal of roentgenology. 2012; 199(1): 8-18. PMid:22733888 http://dx.doi.org/10.2214/AJR.11.7421

[4] Beister M, Kolditz D, Kalender WA. Iterative reconstruction methods in X-ray CT. Physica medica: PM: an international journal devoted to the applications of physics to medicine and biology: official journal of the Italian Association of Biomedical Physics. 2012; 28(2): 94-108. PMid:22316498 http://dx.doi.org/10.1016/j.ejmp.2012.01.003

[5] Chen B, Christianson O, Wilson JM, *et al*. Assessment of volumetric noise and resolution performance for linear and nonlinear CT reconstruction methods. Medical physics. 2014; 41(7): 071909. PMid:24989387 http://dx.doi.org/10.1118/1.4881519

[6] Ghetti C, Palleri F, Serreli G, *et al*. Physical characterization of a new CT iterative reconstruction method operating in sinogram space. Journal of applied clinical medical physics/American College of Medical Physics. 2013; 14(4): 4347. PMid:23835395 http://dx.doi.org/10.1120/jacmp.v14i4.4347.

[7] Li K, Tang J, Chen GH. Statistical model based iterative reconstruction (MBIR) in clinical CT systems: experimental assessment of noise performance. Medical physics. 2014; 41(4): 041906. PMid:24694137 http://dx.doi.org/10.1118/1.4867863

[8] Pontana F, Pagniez J, Duhamel A, *et al*. Reduced-dose low-voltage chest CT angiography with Sinogram-affirmed iterative reconstruction versus standard-dose filtered back projection. Radiology. 2013; 267(2): 609-18.PMid:23297336 http://dx.doi.org/10.1148/radiol.12120414

[9] Siegel MJ, Hildebolt C, Bradley D. Effects of automated kilovoltage selection technology on contrast-enhanced pediatric CT and CT angiography. Radiology. 2013; 268(2): 538-47. PMid:23564712 http://dx.doi.org/10.1148/radiol.13122438

[10] Yu L, Li H, Fletcher JG, *et al*. Automatic selection of tube potential for radiation dose reduction in CT: a general strategy. Medical physics. 2010; 37(1): 234-43. PMid:20175486 http://dx.doi.org/10.1118/1.3264614

[11] Solomon J, Samei E. Quantum noise properties of CT images with anatomical textured backgrounds across reconstruction algorithms: FBP and SAFIRE. Medical physics. 2014; 41(9): 091908. PMid:25186395 http://dx.doi.org/10.1118/1.4893497

[12] Schulz B, Beeres M, Bodelle B, *et al*. Performance of iterative image reconstruction in CT of the paranasal sinuses: a phantom study. AJNR American journal of neuroradiology. 2013; 34(5): 1072-6. PMid:23221946 http://dx.doi.org/10.3174/ajnr.A3339

[13] Samei E, Richard S, Lurwitz L. Model-based CT performance assessment and optimization for iodinated and noniodinated imaging tasks as a function of kVp and body size. Medical physics. 2014; 41(8): 081910. PMid:25086541 http://dx.doi.org/10.1118/1.4890082

[14] Solomon J, Wilson J, Samei E. Characteristic image quality of a third generation dual-source MDCT scanner: Noise, resolution, and detectability. Medical physics. 2015; 42(8): 4941-53 PMid:26233220 http://dx.doi.org/10.1118/1.4923172

[15] Richard S, Husarik DB, Yadava G, *et al*. Towards task-based assessment of CT performance: system and object MTF across different reconstruction algorithms. Medical physics. 2012; 39(7): 4115-22. PMid:22830744 http://dx.doi.org/10.1118/1.4725171

[16] Richard S, Siewerdsen JH. Comparison of model and human observer performance for detection and discrimination tasks using dual-energy x-ray images. Medical physics. 2008; 35(11): 5043-53. PMid:19070238 http://dx.doi.org/10.1118/1.2988161

[17] Burgess AE. Visual perception studies and observer models in medical imaging. Seminars in nuclear medicine. 2011; 41(6): 419-36. PMid:2197844 http://dx.doi.org/10.1053/j.semnuclmed.2011.06.005